www.czasopisma.pan.pl PAN POLSKA AKADEMIA NAUK www.journals.pan.pl

Arch. Metall. Mater. **64** (2019), 2, 451-456

DOI: 10.24425/amm.2019.127559

J. MIETTINEN*, V.-V. VISURI*, T. FABRITIUS*, N. MILCHEVA**, G. VASSILEV***#

THERMODYNAMIC DESCRIPTION OF TERNARY Fe-B-X SYSTEMS. PART 4: Fe-B-V

Thermodynamic descriptions of the ternary Fe-B-V system and its binary sub-system B-V, are developed using experimental thermodynamic and phase equilibrium data from the literature. The thermodynamic parameters of the other binaries, Fe-V and Fe-B, are taken from earlier assessments slightly modifying the Fe-V description. The work is in the context of a new Fe-B-X (X = Cr, Ni, Mn, V, Si, Ti, C) database.

The solution phases are described using substitutional solution model. The borides are treated as stoichiometric or semi-stoichiometric phases and described with two-sublattice models.

Keywords: phase diagrams; thermodynamic modelling; Fe-based systems; Fe-B-X systems thermodynamic database; Fe-B-V system

1. Introduction

The current paper continues our project [1] to develop boron containing iron-based Fe-B-X database, where boron is treated as a substitutional component. The ternary Fe-B-V description follows the optimization of Fe-B-Cr [1], Fe-B-Ni [2], and Fe-B-Mn [3] systems, published earlier in this journal. The goal is to develop a simple and compatible thermodynamic database for steels, which provides important and practical input data for thermodynamic-kinetic models simulating their solidification. The new Fe-B-V description can be applied for modeling of solidification and grain structure formation in various steels [4,5].

The thermodynamic description is for the ternary Fe-B-V system and its binary sub-system, B-V is developed, using the experimental thermodynamic and phase equilibrium data. The latter binary system was assessed in the past [6], but as its unary data differs from that of SGTE (used in this work), which resulted in a reassessment.

The other binary thermodynamic data used in the current Fe-B-V description are taken from [1] for Fe-B and from [7] for Fe-V. The liquid phase description [7], however, was slightly modified in this study, resulting in better agreement with the measured mixing enthalpies.

The Fe-B-V system has been assessed earlier by Homolova et al. [8] where boron was treated as an interstitial constituent and the binary Fe-B and B-V data were different (as mentioned above) from those of the current database. Those discrepancies necessitated a reassessment of the ternary system.

2. Phases, modeling and data

Table 1 shows the phases and their modeling in the current Fe-B-V assessment. The solution phases (L, bcc, fcc) are described with the substitutional solution model. The different borides are treated as stoichiometric phases but a dissolution of the third constituent (i.e mutual substitution between Fe and V atoms) has been allowed where was considered necessary. In agreement with experimental data, no solubility of neither Fe nor Cr in the rhombohedral boron phase (referred to as „bet“

TABLE 1

Phases and their modeling in the current Fe-B-V description

Phase	Modeling
liquid (L)	(B,Fe,V), substitutional, RKM [a]
bcc_A2 (bcc)	(B,Fe,V), substitutional, RKM
fcc_A1 (fcc)	(B,Fe,V), substitutional, RKM
Sigma (σ)	$(Fe)_8(V)_4(Fe,V)_{18}$, sublattice, RKM
Fe_2B (dissolving V)	$(Fe,V)_2(B)$, sublattice, RKM
FeB (dissolving V)	(Fe,V)(B), sublattice, RKM
V_3B_2 (dissolving Fe)	$(Fe,V)_3(B)_2$, sublattice, RKM
VB (dissolving Fe)	(Fe,V)(B), sublattice, RKM
V_3B_4 (dissolving Fe)	$(Fe,V)_3(B)_4$, sublattice, RKM
VB_2 (dissolving Fe)	$(Fe,V)(B)_2$, sublattice, RKM
V_5B_6	$(V)_5(B)_6$, stoichiometric
V_2B_3	$(V)_2(B)_3$, stoichiometric
T-FeVB	$(Fe)_{28}(V)_{32}(B)_{40}$, stoichiometric
beta-rhombo-B (bet)	(B)

[a] – RKM = Redlich-Kister-Muggianu expression (excess Gibbs energy model)

* UNIVERSITY OF OULU, PROCESS METALLURGY RESEARCH UNIT, OULU, FINLAND
** MEDICAL UNIVERSITY OF PLOVDIV, FACULTY OF PHARMACY, PLOVDIV, BULGARIA
*** UNIVERSITY OF PLOVDIV, FACULTY OF CHEMISTRY, PLOVDIV, BULGARIA
# Correspondence address: gpvassilev@excite.com, gpvassilev@gmail.com

bellow) is assumed. A detailed descriptions of the substitutional solution and sublattice models and their adjustable parameters are available [9].

The experimental studies of the Fe-B-V system have been reviewed by Raghavan [10]. Table 2 shows the information selected in the current work. Additionally, the experimental data of Fe-V phase equilibria [11-16], mixing enthalpy in liquid Fe-V alloys [17-19], activities of Fe and V in liquid alloys [20-22], and enthalpy of mixing in bcc alloys [23] were used in the partial re-optimization of the Fe-V system.

TABLE 2

Experimental data applied in the optimizations of the B-V and Fe-B-V systems

System	Experimental data	Reference
B-V	Phase equilibria of the phase diagram Enthalpy of formation of solid alloys, at 25°C	[6], [24] [6]
Fe-B-V	Three isothermal sections, at 1080, 800 and 630°C	[8], [25]

3. Results

The thermodynamic description of the Fe-B-V system is presented in Table 3. The parameters marked with a reference code were taken from earlier assessments and those marked with O* or E*, respectively, were optimized using literature experimental data (Tab. 2) or estimated when no experimental data were available.

The calculated results are compared with the original experimental data to verify the optimization. All calculations were carried out using ThermoCalc software [29].

Figures 1 to 3 show the Fe-B phase diagram calculated by [1] and the Fe-V and B-V phase diagrams calculated in the current study. The agreement with the experimental data is good. The calculated and the experimental invariant points of the B-V system are compared in Table 4.

The main differences between the current calculations of the Fe-V phase diagram and those of Huang [7] can be seen in Figure 1. Namely, the new liquid phase description only slightly changes the bcc+liq equilibrium of the system. Moreover, it has

TABLE 3

Thermodynamic description of the Fe-B-V system. Thermodynamic data of pure components are given by [26,27] unless not shown in the table. Parameter values except for Tc and β are in J/mol

liquid (1 sublattice, sites: 1, constituents: B,Fe,V)	**Ref.**
$L^{L}_{B,Fe} = (-133438+33.946T) + (+7771)(x_B-x_{Fe}) + (+29739)(x_B-x_{Fe})^2$	[28]
$L^{L}_{B,V} = (-183500+12T) + (-108500+45T)(x_B-x_V) + (+60000-2T)(x_B-x_V)^2$	O*
$L^{L}_{Fe,V} = (-40100+5T) + (+1500+5T)(x_{Fe}-x_V)$	O*
bcc (1 sublattice, sites: 1, constituents: B,Fe,V)	
${}^{o}G^{bcc}_{B} = {}^{o}G^{bet}_{B} + (+43514-12.217T)$	[27]
$L^{bcc}_{B,Fe} = (-50000+42T)$	[1]
$L^{bcc}_{B,V} = (-100000+25T)$	O*
$L^{bcc}_{Fe,V} = (-23674+0.465T) + (+8283)(x_{Fe}-x_V)$	[7]
$Tc^{bcc} = 1043x_{Fe}+x_{Fe}x_V(-110+3075(x_{Fe}-x_V)+808(x_{Fe}-x_V)^2-2169(x_{Fe}-x_V)^3)$	[7]
$\beta^{bcc} = 2.22x_{Fe}-2.26x_{Fe}x_V$	[7]
fcc (1 sublattice, sites: 1, constituents: B,Fe,V)	
${}^{o}G^{fcc}_{B} = {}^{o}G^{bet}_{B} + (+50208-13.478T)$	[27]
$L^{fcc}_{B,Fe} = (-66000+50T)$	[1]
$L^{fcc}_{B,V} = L^{bcc}_{B,V}$ (fcc not stable in binary B-V)	E*
$L^{fcc}_{Fe,V} = (-15291-4.138T)$	[7]
$Tc^{fcc} = -201x_{Fe}$	[26]
$\beta^{fcc} = -2.1x_{Fe}$	[26]
Sigma (σ) (3 sublattices, sites: 8:4:18, constituents: Fe:V:Fe,V)	
${}^{o}G^{\sigma}_{Fe:V:Fe} = 8{}^{o}G^{fcc}_{Fe}+4{}^{o}G^{bcc}_{V}+18{}^{o}G^{bcc}_{Fe} + (-157961+60.729T)$	[7]
${}^{o}G^{\sigma}_{Fe:V:V} = 8{}^{o}G^{fcc}_{Fe}+22{}^{o}G^{bcc}_{V} + (-205321-60.967T)$	[7]
$L^{\sigma}_{Fe:V:Fe,V} = (-305784)$	[7]
Fe_2B (2 sublattices, sites: 0.6667:0.3333, constituents: Fe,V:B)	
${}^{o}G^{Fe2B}_{Fe:B} = 0.6667{}^{o}G^{bcc}_{Fe}+0.3333{}^{o}G^{bet}_{B} + (-26261+3.466T)$	[26]
${}^{o}G^{Fe2B}_{V:B} = 0.6667{}^{o}G^{bcc}_{V}+0.3333{}^{o}G^{bet}_{B} + (-15000+5T)$	O*
$L^{Fe2B}_{Fe,V:B} = (-84000+20T)$	O*
FeB (2 sublattices, sites: 0.5:0.5, constituents: Fe:B)	
${}^{o}G^{FeB}_{Fe:B} = 0.5{}^{o}G^{bcc}_{Fe}+0.5{}^{o}G^{bet}_{B} + (-35150+6T)$	[1]
${}^{o}G^{FeB}_{V:B} = 0.5{}^{o}G^{bcc}_{V}+0.5{}^{o}G^{bet}_{B} + (-15000+5T)$	O*
$L^{FeB}_{Fe,V:B} = (-68000)$	O*

V_3B_2 (2 sublattices, sites: 0.6:0.4, constituents: Fe,V:B)	
${}^oG^{V3B2}_{Fe:B} = 0.6{}^oG^{bcc}_{Fe}+0.4{}^oG^{bet}_{B} + (-15000+5T)$	O*
${}^oG^{V3B2}_{V:B} = 0.6{}^oG^{bcc}_{V}+0.4{}^oG^{bet}_{B} + (-56070+1.67T)$	[6]
$L^{V3B2}_{Fe,V:B} = (-41500)$	O*
VB (2 sublattices, sites: 0.5:0.5, constituents: Fe,V:B)	
${}^oG^{VB}_{Fe:B} = 0.5{}^oG^{bcc}_{Fe}+0.5{}^oG^{bet}_{B} + (-15000+5T)$	O*
${}^oG^{VB}_{V:B} = 0.5{}^oG^{bcc}_{V}+0.5{}^oG^{bet}_{B} + (-69134+2.51T)$	[6]
$L^{VB}_{Fe,V:B} = (-19000)$	O*
V_3B_4 (2 sublattices, sites: 0.429:0.571, constituents: Fe,V:B)	
${}^oG^{V3B4}_{Fe:B} = 0.429{}^oG^{bcc}_{Fe}+0.571{}^oG^{bet}_{B} + (-24000+5T)$	O*
${}^oG^{V3B4}_{V:B} = 0.429{}^oG^{bcc}_{V}+0.571{}^oG^{bet}_{B} + (-70290+2.85T)$	[6]
$L^{V3B4}_{Fe,V:B} = (-24000)+(-19000)(y_{Fe}-y_V)$	O*
VB_2 (2 sublattices, sites: 0.333:0.667, constituents: Fe,V:B)	
${}^oG^{VB2}_{Fe:B} = 0.333{}^oG^{bcc}_{Fe}+0.667{}^oG^{bet}_{B} + (-15000+5T)$	O*
${}^oG^{VB2}_{V:B} = 0.333{}^oG^{bcc}_{V}+0.667{}^oG^{bet}_{B} + (-67853+3.35T)$	[6]
$L^{VB2}_{Fe,V:B} = (-11000)$	O*
V_5B_6 (2 sublattices, sites: 0.455:0.545, constituents: V:B)	
${}^oG^{V5B6}_{V:B} = 0.455{}^oG^{bcc}_{V}+0.545{}^oG^{bet}_{B} + (-70116+2.85T)$	[6]
V_2B_3 (2 sublattices, sites: 0.4:0.6, constituents: V:B)	
${}^oG^{V2B3}_{V:B} = 0.4{}^oG^{bcc}_{V}+0.6{}^oG^{bet}_{B} + (-69856+3.05T)$	[6]
T-FeVB (3 sublattices, sites: 0.28:0.32:0.40, constituents: Fe:V:B)	
${}^oG^{T}_{Fe:V::B} = 0.28{}^oG^{bcc}_{Fe}+0.32{}^oG^{bcc}_{V}+0.40{}^oG^{bet}_{B} + (-50000-9.7T+1.5TlnT)$	O*

O* – Parameter optimized in this work; E* – Parameter estimated in this work

a small effect on the calculated [7] Fe and V activities in liquid phase, which agrees reasonably well with the experimental data [20-22]. However, the new liquid phase description noticeably improves the agreement with the experimental enthalpy data of mixing in liquid [17-19], as shown in Figure 4.

A good conformity was obtained also between the calculated and the experimental bcc+fcc region [13,14] (indistinct in Figure 2) and the enthalpy of mixing of bcc alloys [23]. In these two cases, the results were identical to those of Huang [7].

Another result for the binary B-V system is presented in Figure 5. It shows the calculated enthalpy of formation of solid B-V alloys at 25°C, which agrees well with the experimental data of Spear et al. [6].

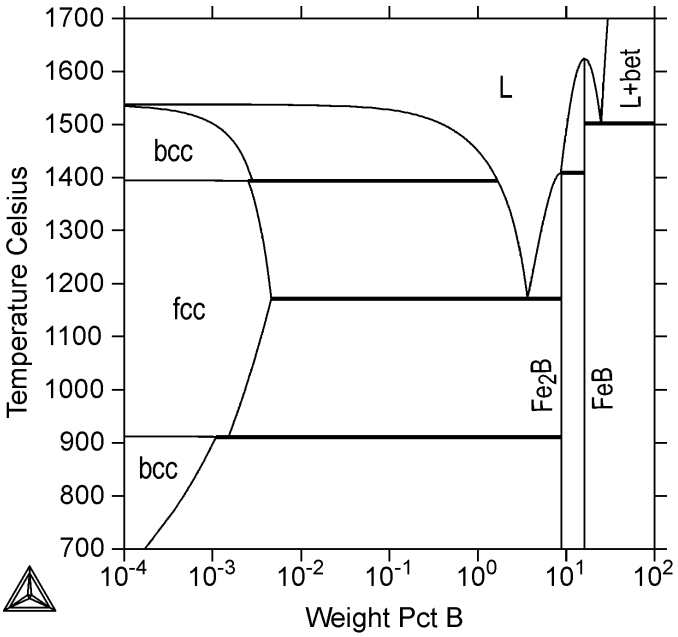

Fig. 1. Calculated [1] Fe-B phase diagram

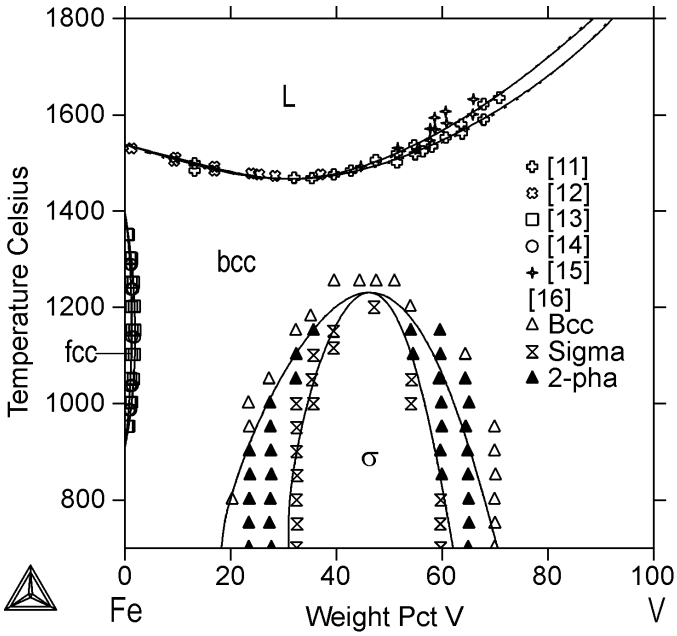

Fig. 2. Calculated Fe-V phase diagram, together with experimental data points [11-16] Solid lines refer to the current calculations and dotted lines refer to those of [7]

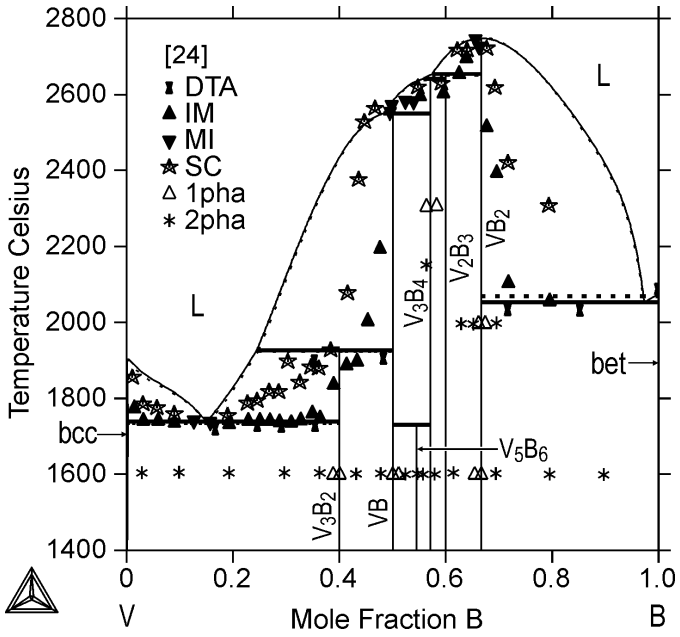

Fig. 3. Calculated B-V phase diagram, together with experimental data points [24]. DTA – differential thermal analysis, IM – incipient melting, MI – melted isothermally and SC – specimen collapsed. Solid lines refer to the current calculations and dotted lines refer to those of [6]

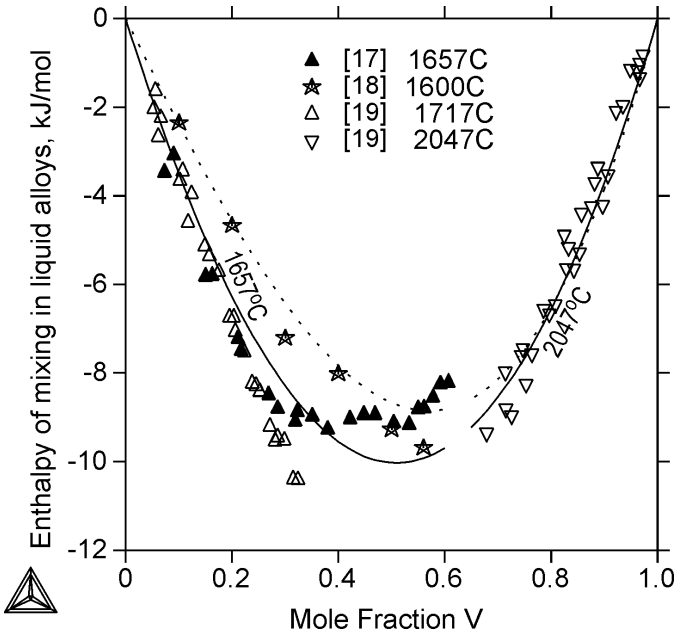

Fig. 4. Calculated enthalpy of mixing of liquid Fe-V alloys at 2047°C and 1657°C, together with experimental data points [17-19]. Solid lines refer to the current calculations and dotted lines refer to those of [7]. The reference states used are pure liquid Fe and V

TABLE 4

Calculated (calc) and experimental (exp) invariant points of the B-V system. $C_B^{\phi i}$ denotes the B concentration (wt%) in a equilibrium phase ϕi; t – temperature, °C

ϕ1 – ϕ2 – ϕ3	**t °C**	**$C_B^{\phi 1}$ wt%**	**$C_B^{\phi 2}$ wt%**	**$C_B^{\phi 3}$ wt%**	**Reference**
L = bcc+V_3B_2	1739 1737	3.60 3.34	0.05 <0.21	12.39 12.39	calc this study exp [24]
L+VB = V_3B_2	1926 1900	6.43 6.94	17.51 17.51	12.39 12.39	calc this study exp [24]
L+V_3B_4 = VB	2551 2570	16.58 16.94	22.02 21.95	17.51 18.09	calc this study exp [24]
VB+V_3B_4 = V_5B_6	1729 1727	17.51 17.51	22.02 21.95	20.27 20.27	calc this study exp [6]
L+V_2B_3 = V_3B_4	2641 2610	21.13 19.94	24.15 24.15	22.02 21.26	calc this study exp [24]
L+VB_2 = V_2B_3	2654 2667	22.27 21.95	29.83 30.11	24.15 24.15	calc this study exp [6]
L = VB_2	2748 2747	29.83 29.18	29.83 29.18	—	calc this study exp [24]
L = VB_2+bet	2053 2035	88.50 91.23	29.83 31.08	100 100	calc this study exp [24]

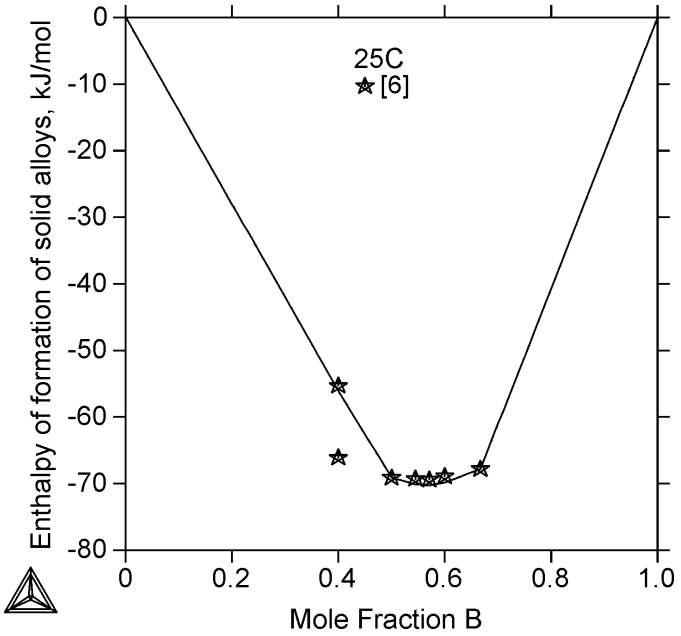

Fig. 5. Calculated enthalpy of formation of solid B-V alloys at 25°C, together with experimental data points [6]. Calculations of are practically identical to those of [6]. The reference states used are pure bcc V and pure beta-rhombo B

The results for the Fe-B-V system are represented in Figs. 6 to 10. The calculated liquidus projection (Fig. 6) should be considered as highly tentative due to the lack of ternary experimental data for the liquid phase. This statement also applies the recent Fe-B-V description of Homolova et al. [8].

Figs. 7 to 9 show three isothermal sections of the system (at 1080, 800 and 630°C, respectively). The calculations agree reasonably well with the measurements of Homolova et al. [8] at 1080 and 630°C, and with those of Kuzma and Starodub [25] at 800°C. The calculated results are very similar with [8]. The main differences is the higher solubility of Fe in V_2B_3 considered in the current work, which agrees better with the measurements of [25], and the higher solubility of V in Fe_2B, which agrees not that well with the same measurements (Fig. 8). The ternary T phase, observed by [8] but not detected by [25] does not appear at 800°C (Fig. 8) as we retained the latter results. The reason is

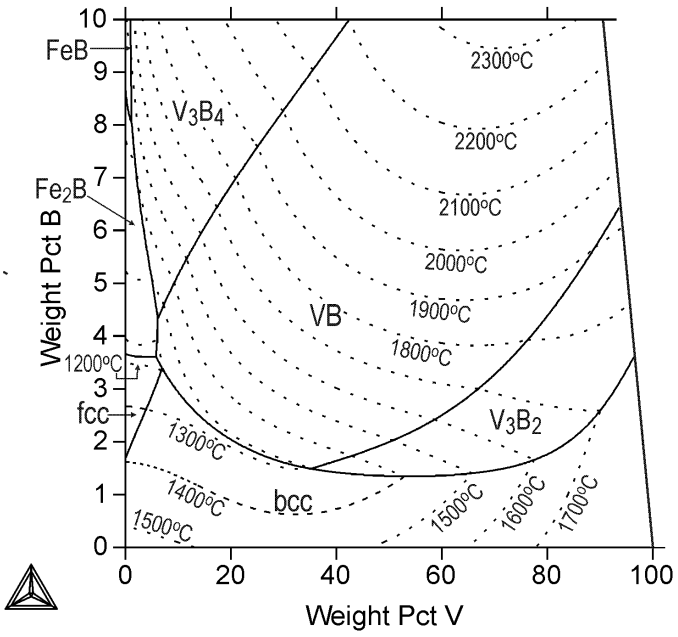

Fig. 6. Calculated liquidus projection of the Fe-B-V system. The calculated liquidus isotherms between 1200 and 2300°C (dotted lines) are shown too

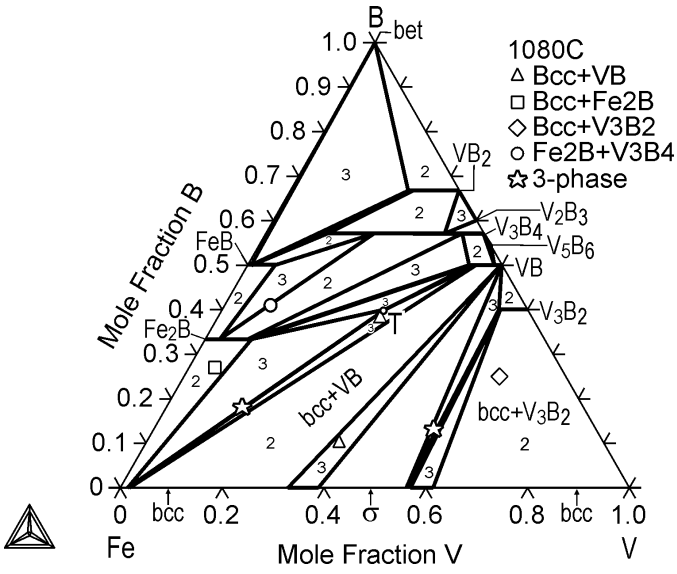

Fig. 7. Calculated isotherm of 1080°C in the Fe-B-V system, together with experimental data points [8]. The calculated two-phase and three-phase regions are indicated by numbers 2 and 3, respectively. The fcc phase was suspended from the calculations for the sake of clarity

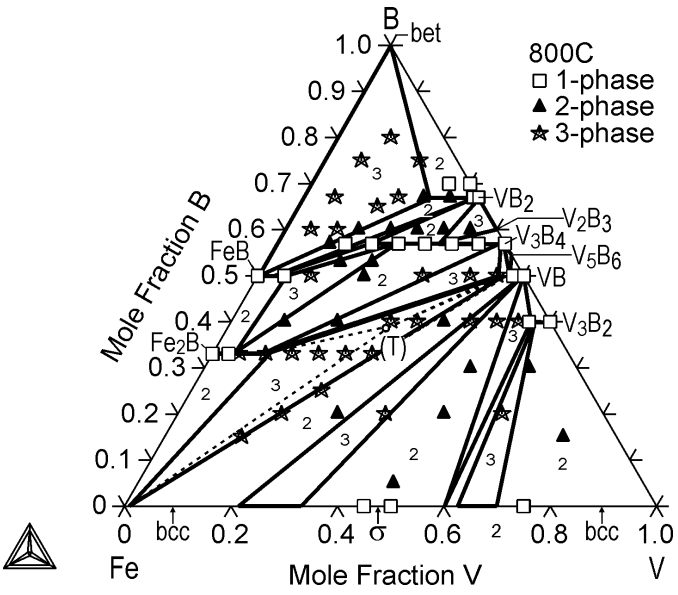

Fig. 8. Calculated isotherm of 800°C in the Fe-B-V system, together with experimental data points [25]. The calculated two-phase and three-phase regions are indicated by numbers 2 and 3, respectively. The ternary T phase was suspended from calculations as not detected by [25]

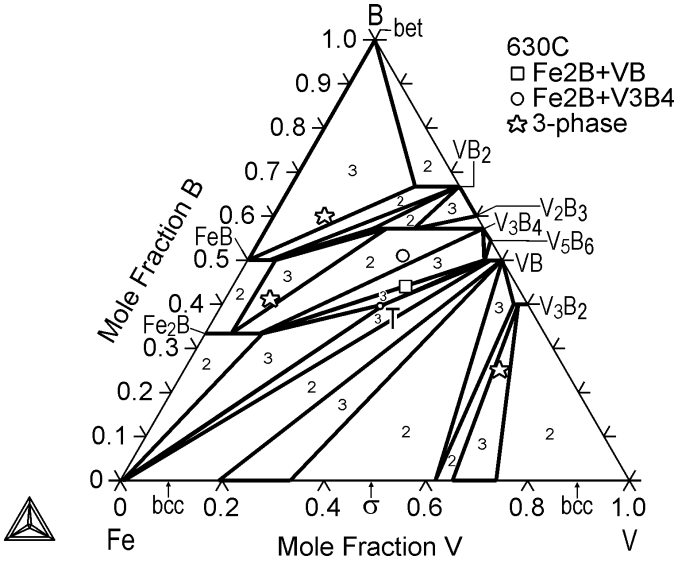

Fig. 9. Calculated isotherm of 630°C in the Fe-B-V system, together with experimental data points [8]. The calculated two-phase and three-phase regions are indicated by numbers 2 and 3, respectively

that the existence of the new phase was suggested considering other phase equilibria. Nevertheless, the dotted lines in Fig. 8 show that its inclusion would only slightly change the phase relations. The ternary T phase forms new equilibria in a very limited region within the triangle bcc-Fe_2B-VB (Fig. 8). Apparently, the stability of the T phase would be barely higher than those of the neighboring phases, which explains why it was not found by Kuzma and Starodub [25]. Furthermore, they did not identify the phase equilibria precisely, but listed only the number of the phases taking part in different equilibria.

Figure 10 shows the calculated boron solubility in the bcc and the fcc phases. The V content increase promotes the VB and T phases formation, which slightly decreases the boron solubility. That solubility is decreased also by the temperature drop from 1150 to 1000°C.

4. Summary

The equilibria between fourteen phases (liquid, bcc, fcc, sigma, Fe_2B, FeB, V_3B_2, VB, V_3B_4, VB_2, V_5B_6, V_2B_3, T-FeVB

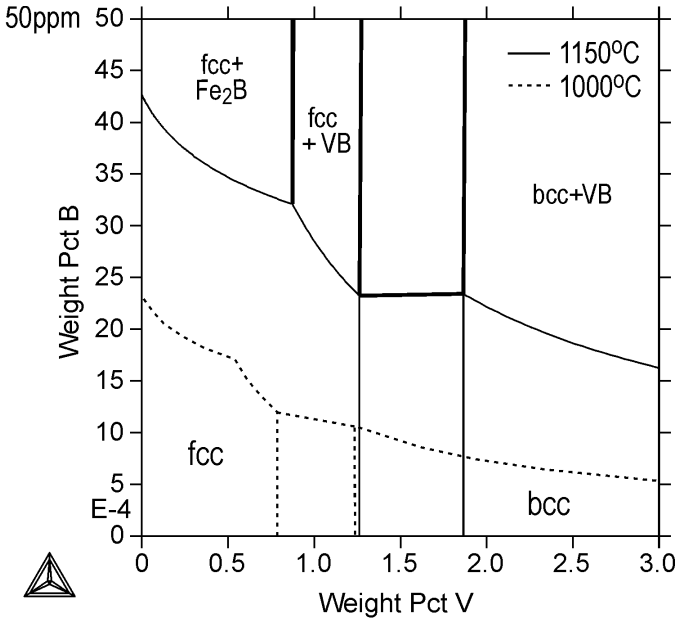

Fig. 10. Calculated B solubility in the fcc and bcc phases of the Fe-B-V system, at 1150 and 1000°C

and beta-rhombo-B (bet)) belonging to the ternary Fe-B-V phase diagram and the respective binary systems were considered. Thermodynamic optimizations of the ternary Fe-B-V and the binary B-V system were performed. A slight modification of the liquid Fe-V phase description has been done as well.

Good or reasonable correlation was obtained between the calculated and the experimental thermodynamic and phase equilibrium data. However, experimental measurements of the ternary liquid phase are necessary before a reliable description of the primary liquid surfaces of the system is developed. Clearly, if such data become available, one has to optimize the liquid phase description as well as some of the current boride phase descriptions, as most borides form equilibria with the liquid phase.

Acknowledgement

This study was executed within the framework of the Genome of Steel profiling project, by Dr. J. Miettinen, Dr. V-V. Visuri and Prof. T. Fabritius.

REFERENCES

[1] J. Miettinen, G. Vassilev, Arch. Metall. Mater. **59**, 601 (2014).
[2] J. Miettinen, G. Vassilev, Arch. Metall. Mater. **59**, 609 (2014).
[3] J. Miettinen, K. Lilova, G. Vassilev, Arch. Metall. Mater. **59**, 1481 (2014).
[4] J. Miettinen, S. Louhenkilpi, H. Kytönen, J. Laine, Math. Comput. Simulat. **80**, 1536 (2010)
[5] A. Burbelko, J. Falkus, W. Kapturkiewicz, K. Solek, P. Drozdz, M. Wrobel, Arch. Metall. Mater. **57**, 379 (2012).
[6] K.E. Spear, P.K. Liao, J.F. Smith, Bull. Alloy Phase Diagrams **8**, 447 (1987).
[7] W. Huang, Z. Metallkd. **82**, 391 (1991).
[8] V. Homolova, A. Kroupa, A. Vyrostkova, J. Alloy Compd. **520**, 30 (2012).
[9] C. Qiu, Thermodynamic study of carbon and nitrogen in stainless steels. PhD thesis, Royal Institute of Technology, Stockholm (1993).
[10] V. Raghavan, Phase Diagrams of Ternary Iron Alloys – Part **6A**, Indian Institute of Metals, Calcutta, 440 (1992).
[11] F. Wever, W. Jellinghaus, Mitt. Kaiser-Wilhelm Inst. Eisenforsch., Düsseldorf, **12**, 317 (1930).
[12] A. Hellawell, W. Hume-Rothery: Phil. Trans. Roy. Soc. London, **A249**, 417 (1957).
[13] W.A. Fischer, K. Lorenz, H. Fabritius, D. Schlegel, Arch. Eisenhüttenwes. **41**, 489 (1970).
[14] G. Kirchner, G. Gemmel, Report Dept. of Physical Metallurgy, Royal Institute of Technology, Stockholm, Sweden (1970).
[15] T. Furukawa, E. Kato, Tetsu-to-Hagane **61**, 3050 (1975).
[16] K. Hack, H.D. Nüssler, J. Spencer, G. Inden, Proc. CALPHAD VIII, Royal Institute of Technology, Stockholm, Sweden (1979).
[17] G.L. Batalin, V.S. Sudavtsova, Yu.K. Vysotskij, Izv. Akad. Nauk SSSR, Met. **6**, 52 (1982).
[18] Y. Iguchi, S. Nobori, K. Saito, T. Fuwa, Tetsu-to-Hagane **68**, 633 (1982).
[19] K. Schaefers, J. Qin, M.G. Frohberg, Steel Research **64**, 229 (1993).
[20] C.W. Weidner, Jr, PhD Thesis, Ohio State Univ. (1971).
[21] E. Kato, T. Furukawa, in: The Fourth Japan-USSR Joint Symposium on Physical Chemistry of Metallurgical Processes, Iron and Steel Institute of Japan, 201 (1973).
[22] O. Kubaschewski, H. Probst, K.H. Geiger, Z. Phys. Chem. Neue Folge **104**, 23 (1977).
[23] P.J. Spencer, F.H. Putland, J. Iron Steel Inst. **211**, 293 (1973).
[24] E. Rudy, USAF Tech. Report AFML-TR-65-2. Part **V**, Wright Patterson AFB, OH (1969).
[25] Yu. Kuzma, P. Starodub, Inorg. Mater. **9**, 337 (1973).
[26] A.T. Dinsdale, SGTE unary database, version 4.4; www.sgte.org.
[27] I. Ansara, A.T. Dinsdale, M.H. Rand, COST 507 – Thermochemical database for light metal alloys, Volume **2**, European Communities, Belgium (1998).
[28] B. Hallemans, Wollants, J.R. Roos, Z. Metallkd. **85**, 676 (1994).
[29] J.-O. Andersson, T. Helander, L. Höglund, P. Shi, B. Sundman, CALPHAD **26**, 273 (2002).